Strong correlation between the cation ordering and magnetic properties of anodically electrodeposited Mn–Co–O nanocrystals

Weifeng Wei · Mehmet Egilmez · Weixing Chen ·
Jan A. Jung · Douglas G. Ivey

Abstract The rock salt-to-spinel structural transformation that occurs in anodically electrodeposited Mn–Co–O nanocrystals involves a rearrangement of Mn/Co cations from octahedral interstices to tetrahedral interstices. The cation ordering process leads to distinct magnetic properties. Curie temperature (T_C) and blocking temperature (T_B) increase dramatically with annealing temperature (200–400 °C), while the corresponding change in particle size for the oxide nanocrystals is rather small. A strong correlation between the magnetic properties and the cation ordering degree in annealed Mn–Co–O nanocrystals was established. These unique magnetic properties can be attributed to the magnetic moment changes induced by Mn/Co cation ordering from octahedral interstices to tetrahedral interstices in the annealed Mn–Co oxide nanocrystals.

Introduction

Transition metal oxide nanocrystals possess distinct morphologies, crystal structures, cation distributions, and oxidation states in comparison with the corresponding bulk materials, which may introduce novel and/or improved

W. Wei · W. Chen · D. G. Ivey (✉)
Department of Chemical and Materials Engineering,
University of Alberta, Edmonton, AB T6G 2V4, Canada
e-mail: doug.ivey@ualberta.ca

M. Egilmez · J. A. Jung
Department of Physics, University of Alberta, Edmonton,
AB T6G 2G7, Canada

W. Wei
Department of Materials Science and Engineering,
Massachusetts Institute of Technology, Cambridge,
MA 02139, USA

physicochemical properties [1, 2]. Recently, one class of promising functional materials, magnetic oxide nanocrystals (e.g., MnO, Mn_3O_4, CoO, Co_3O_4, NiO, and $CoMn_2O_4$) have been extensively investigated owing to their importance in fundamental research and a wide variety of potential technological applications [3–15]. In these magnetic oxide nanocrystals, anomalous magnetic properties, such as the divergence between zero-field cool (ZFC) and field cool (FC) magnetization and magnetic hysteresis below the blocking temperature (T_B), have been demonstrated. The magnetic anomalies are normally attributed to uncompensated surface spins causing a change in the magnetic order in the oxide nanocrystals [3–15]. However, it is noted that the magnetic properties of magnetic oxide nanocrystals are rather sensitive to their size, morphology, and crystal chemistry, so that scattered or even contradictory magnetic data have been reported for the same oxide nanocrystals such as MnO [3–7].

Contrary to the high-crystallization degree of the oxide nanocrystals prepared by chemical routes [3–15], it has been demonstrated in our previous studies [16, 17] that Mn–Co–O nanocrystals synthesized through electrochemical methods have a defective rock salt-type structure. In this metastable rock salt structure, in addition to the metal cations (Co and/or Mn), a significant number of vacancies reside in the octahedral interstices of the face-centered cubic (FCC) arrays of oxygen anions [17]. When annealed at high temperatures, the defective rock salt structure gradually transformed into the stable spinel structure [18]. The structural transformation involved the migration of Mn/Co cations from octahedral interstices to tetrahedral interstices, which was accompanied by the reduction of Mn/Co cations and oxygen evolution. In this work, we demonstrate the effect of crystal chemistry evolution (i.e., cation ordering process) on the magnetic properties of

Mn–Co–O nanocrystals during the rock salt-to-spinel structural transformation. It is expected that these experimental findings may enhance the knowledge base for understanding the complex magnetic properties of transition metal oxide nanocrystals.

Experimental procedures

Mn–Co oxide nanocrystals were deposited on Au-coated Si wafers using an anodic electrodeposition process, as described previously [16]. The solutions consisted of 0.2 M EDTA disodium and various concentrations of $CoSO_4 \cdot 7H_2O$ and $MnSO_4 \cdot H_2O$. The total metal ion concentration in the solutions was set to 0.3 M. Two Co(II)/Mn(II) mole ratios (29:1 and 9:1) in the solutions were used to obtain two types of mixed Mn–Co–O nanocrystals: Co-rich and Mn-rich samples. The deposition current density, pH value, and solution temperature were adjusted to be 5 mA/cm^2, 6.0, and 70 °C, respectively. The chemical formulae for the as-deposited Co-rich and Mn-rich oxide nanocrystals were determined to be $Mn_{1.2}Co_{1.22}O_4$ and $Mn_{2.2}Co_{0.1}O_4$ using wavelength dispersive spectroscopy (WDS), which are consistent with the results in a previous study [17]. Heat treatment of the as-deposited Mn–Co–O nanocrystals was conducted in air at various temperatures ranging from 100 to 500 °C, for 5 h.

Quantitative chemical analysis of the Mn–Co–O nanocrystals was conducted using a JEOL 8900 microprobe, equipped with five wavelength dispersive spectrometers (WDS). The microprobe was operated at an energy of 15 kV with a beam current of 15 nA. The quantitative information for each sample was obtained by averaging ten independent measurements. The crystal structure and morphology of the annealed Mn–Co–O nanocrystals were investigated using transmission electron microscopy (TEM). Crystal structure analysis was performed using selected area diffraction (SAD) patterns obtained from the thinnest regions. Electron transparent samples were produced by scraping off the deposits, mechanically grinding, and ultrasonically dispersing in methanol. One or two drops of the suspension were then deposited on carbon-coated Cu grids. After evaporation of the methanol, samples were ready for analysis. Electron diffraction and imaging were performed in a JEOL 2010 transmission electron microscope (TEM) operated at 200 kV, equipped with a Noran ultra-thin window (UTW) X-ray detector.

Magnetic property measurements for the Mn–Co oxide nanocrystals were performed with a superconducting quantum interference device (SQUID) magnetometer (Quantum Design) in direct current (DC) mode. The oxide nanocrystals deposited on the Au-coated Si wafers were scraped off and placed into plastic capsules, which were mounted inside the plastic straws during magnetic measurements. The magnetization measured from the empty (diamagnetic) plastic straw was subtracted as background from the obtained magnetization of the oxide samples. The mass of the oxide nanocrystals in the plastic capsules was determined with a microbalance with an accuracy of 10 μg (Sartorius BP211D). The mass loading of the oxide samples measured in the SQUID was within the range of 0.0035 to 0.005 g. The temperature dependent magnetization measurements were conducted between 10 and 250 K. All the magnetic measurements were carried out in a field of 100 Gauss.

Results and discussion

Morphology and crystal structure of Mn–Co–O nanocrystals annealed at different temperatures

Figure 1 shows representative TEM micrographs, corresponding SAD patterns, and grain size distributions for electrodeposited Mn–Co–O nanocrystals annealed at various temperatures. Based on the SAD patterns, it is apparent that both the Mn-rich and Co-rich Mn–Co oxide nanocrystals maintain the single phase, rock salt-type structure when the annealing temperatures do not exceed 400 °C. Upon careful examination of the SAD patterns, it is noted that the lattice parameters (a) of the rock salt-type unit cell decrease steadily as the annealing temperature is raised from 100 to 400 °C. For Mn-rich oxide nanocrystals, the lattice parameters are 0.439 nm (100 °C), 0.436 nm (200 °C), 0.431 nm (300 °C), and 0.428 nm (400 °C), whereas the corresponding lattice parameters for Co-rich oxide nanocrystals are 0.428 nm (100 °C), 0.426 nm (200 °C), 0.420 nm (300 °C), and 0.416 nm (400 °C), respectively. The rock salt-to-spinel structural transformation occurs in oxide nanocrystals annealed at a temperature of 500 °C. A cubic $Fd3m$ spinel-type structure was obtained in the Co-rich, Mn–Co–O oxide nanocrystals, while a distorted tetragonal-type spinel phase with space group of $I4_1/amd$ formed in the Mn-rich oxide nanocrystals, which is consistent with previous results [18]. It should be noted that structural changes occur at temperatures below 500 °C, as indicated by the lattice parameter changes on annealing from 100 to 400 °C. It is apparent from the TEM micrographs that the oxide nanocrystals are quite equiaxed. A size distribution analysis was conducted on TEM micrographs taken from different regions in each nanocrystalline sample, using Image Pro Plus 6.0 software. The size of an oxide particle can be obtained by averaging the length of the diameters passing through the particle's centroid measured at 2° intervals. As the annealing temperature is increased from 100 to 500 °C, the average particle sizes for the Mn-rich nanocrystals are 5.6 (100 °C),

Fig. 1 TEM micrographs, SAD patterns, and particle size distributions for oxide nanocrystals annealed at various temperatures. **a** Mn-rich sample annealed at 100 °C; **b** Co-rich sample annealed at 100 °C; **c** Mn-rich sample annealed at 400 °C; **d** Co-rich sample annealed at 400 °C; **e** Mn-rich sample annealed at 500 °C; **f** Co-rich sample annealed at 500 °C. Note that (**a**)–(**d**) are dark field (DF) images
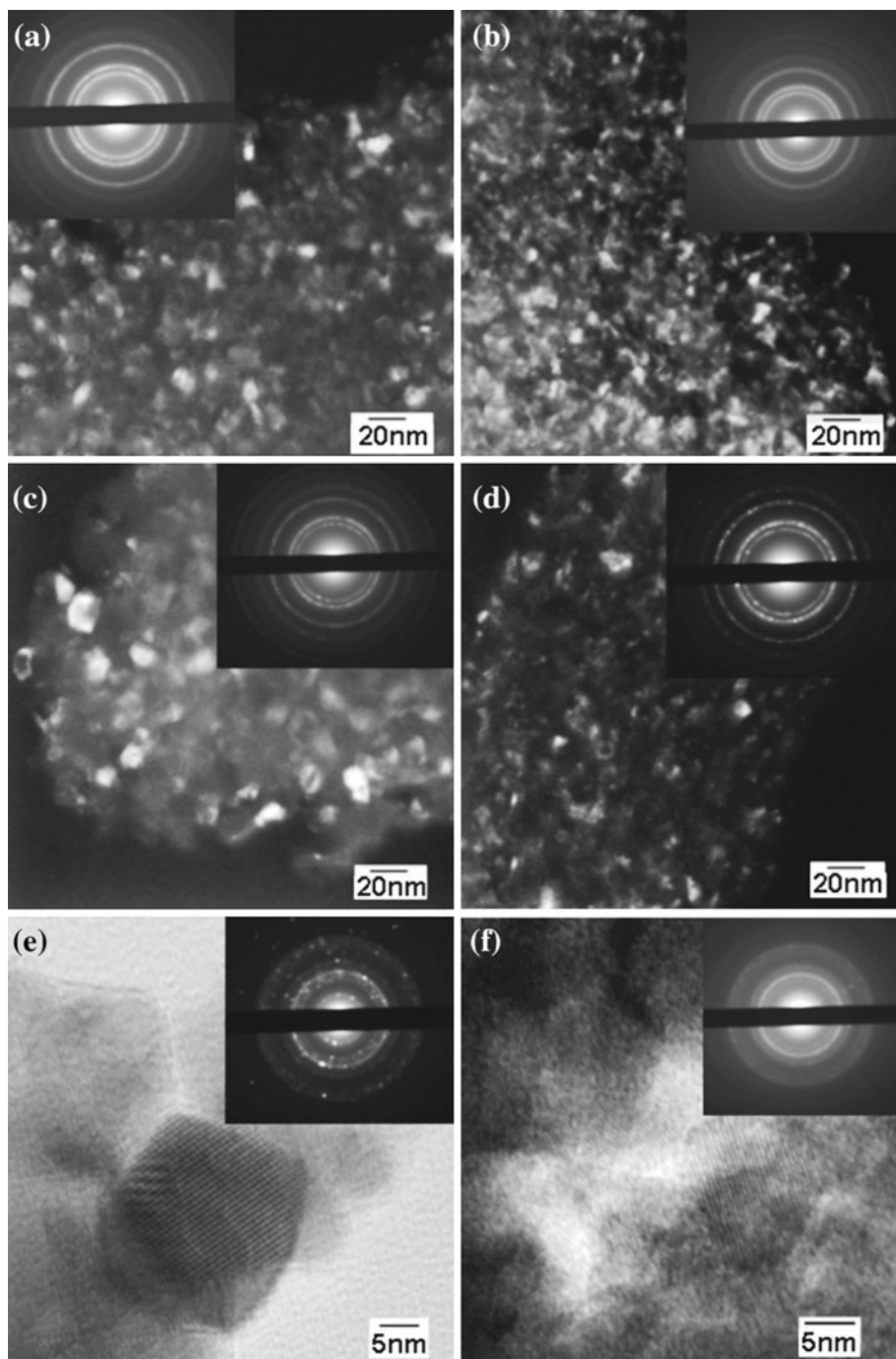

5.9 (200 °C), 6.0 (300 °C), 10.1 (400 °C), and 22.0 nm (500 °C), while the mean sizes for the Co-rich nanocrystals are 3.4 (100 °C), 3.6 (200 °C), 4.3 (300 °C), 4.6 (400 °C), and 16.0 nm (500 °C), respectively.

Magnetic properties of Mn–Co–O nanocrystals annealed at different temperatures

Figure 2 shows the temperature dependence for ZFC and FC magnetization for the Mn–Co–O nanocrystals treated at various temperatures. All the measurements were carried out in a field of 100 Gauss. The ZFC and FC magnetization curves for the Mn–Co oxide nanocrystals annealed at 100 °C are fully reversible between 10 and 250 K (insets in Fig. 2a, b). Corresponding magnetization magnitudes are relatively small, indicative of typical paramagnetic behavior, which is further confirmed by the corresponding inverse magnetization curves in Fig. 2c, d. When the annealing temperatures range from 200 to 500 °C, however, an irreversible phenomenon exists between the ZFC
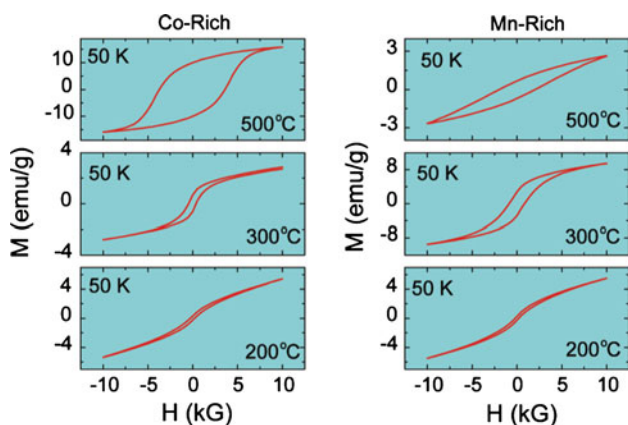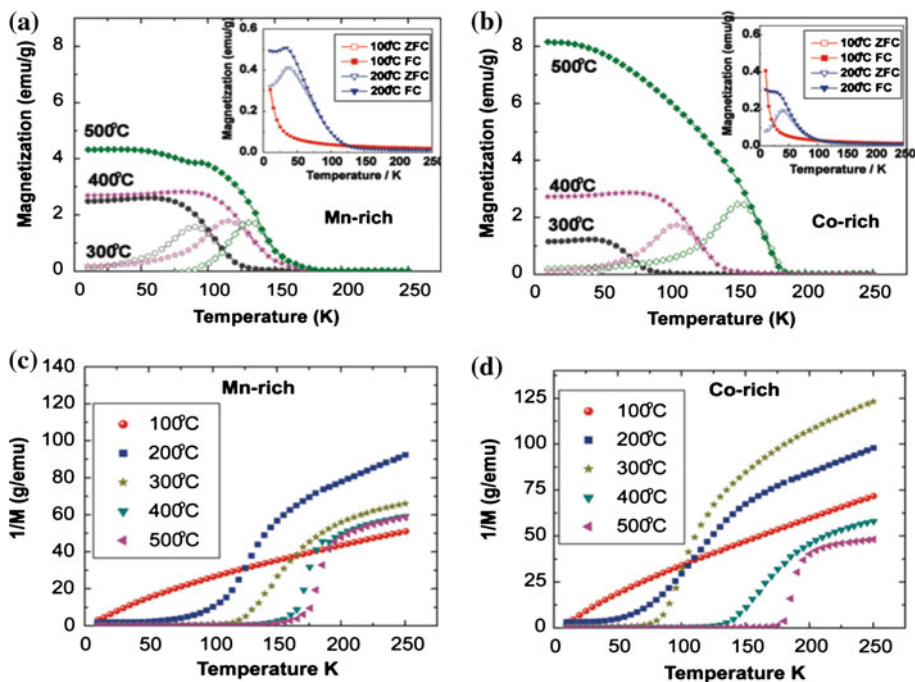
Fig. 3 Hysteresis curves for Co-rich and Mn-rich oxide nanocrystals
annealed at various temperatures ranging from 200 to 500 °C. The
measurement temperature was 50 K

and FC magnetization curves, as shown in Fig. 2a, b.
Figure 3 shows the field dependence of magnetization
(hysteresis curves) for samples prepared at 200, 300, and
500 °C at a temperature of 50 K. As evident from the
ferromagnetic hysteresis in Fig. 3, the rise in the temperature
dependence of DC magnetization (Fig. 2a, b) is
attributed to the onset of the ferromagnetic behavior in the
samples annealed at temperatures from 200 to 500 °C. The
coercive field increases from 150 to 3,600 Gauss and from
170 to 2,000 Gauss for Co-rich and Mn-rich samples,
respectively. The large discrepancy between the ZFC and
FC magnetization curves below the Curie temperature (T_C)
reveals a characteristic superparamagnetism. This kind of
magnetic behavior is expected in very fine ferromagnetic

particles. In such systems, due to the reduced size of the
ferromagnetic crystallite, the thermal energy is sufficient to
change the direction of the magnetization of the entire
crystallite [19]. The blocking temperature (T_B) is the
threshold point of thermal activation. Above T_B, mag-
netocrystalline anisotropy is overcome by thermal activa-
tion and the magnetization direction of each nanoparticle
simply follows the applied field direction. Consequently,
the nanoparticles show paramagnetic properties. From the
inverse magnetizations curves in Fig. 2c, d, an intriguing
magnetic behavior is also observed in those samples
annealed at temperatures ranging from 200 to 500 °C. The
inverse magnetization curves show a deviation from the
Curie–Weiss law, similar to that observed in ferromagnets
with short-range ferromagnetic correlations above the
Curie temperature [20, 21]. This kind of deviation in the
samples indicates the presence of an intrinsic magnetically
inhomogeneous paramagnetic state, namely short-range
ferromagnetic clusters persist above the magnetic ordering
temperature.

The Curie temperature of the oxide nanocrystals is
determined from the minimum of the temperature depen-
dence of dM/dT, which corresponds very closely to the
onset of the increase in magnetization M. Curie tempera-
tures are plotted as a function of oxide particle size in
Fig. 4a, b. It is observed that larger oxide particles have
higher T_C, but do not follow a linear trend with the particle
size changes. For Mn-rich oxides annealed at temperatures
from 200 to 400 °C, T_C increases from 56 to 128 K, while
the corresponding change in average particle size of the
oxide nanocrystals is rather small (increases from 5.9 to
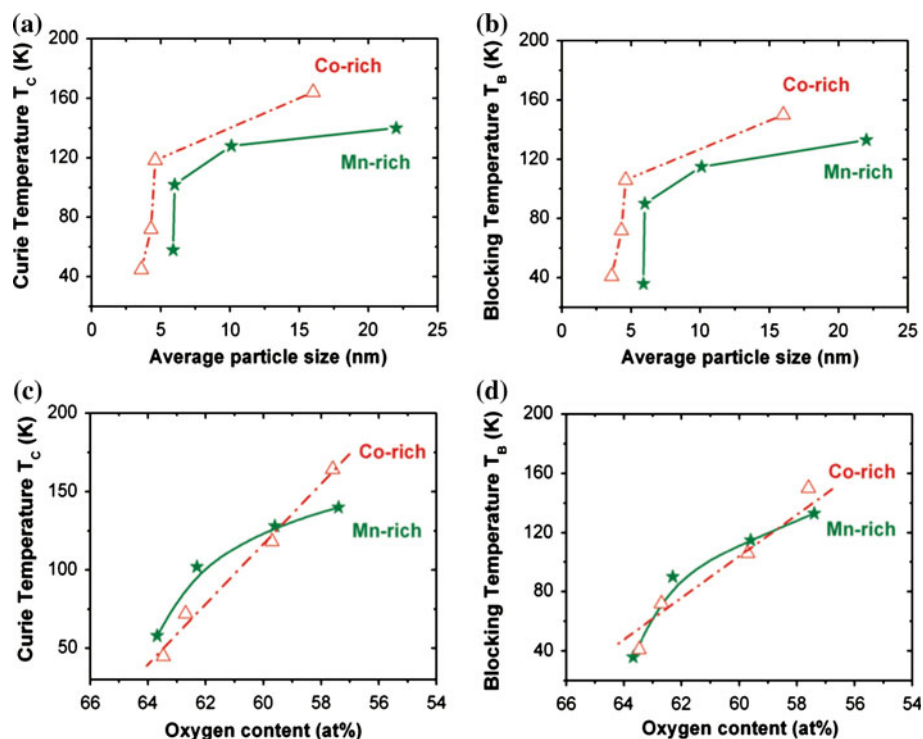
10.1 nm). For the Co-rich counterparts, T_C increases from 40 to 117 K, but the corresponding particle size growth from 3.6 to 4.6 nm is negligible. As discussed earlier, one expected behavior is the presence of superparamagnetism (spontaneous rotation of the magnetization of the samples) in these oxide nanocrystals. The blocking temperature (T_B) is determined from the peak of each ZFC magnetization curve. Figure 4a, b present the blocking temperature as a function of oxide particle size. It is apparent that T_B also increases rapidly with annealing temperature (200–400 °C), while the corresponding particle size growth of the oxide nanocrystals is rather small, especially for Co-rich oxide nanocrystals. In addition to the oxide particle size, therefore, the crystal chemistry evolution of the oxide nanocrystals after annealing has to be taken into account to understand their distinct magnetic behavior.

Correlation between cation ordering and the magnetic properties

It has been shown that the structural transformation of rock salt-type Mn–Co oxide to spinel-type Mn–Co oxide involves a rearrangement of cations (Mn/Co) from octahedral interstices to tetrahedral interstices, which is accompanied by cation reduction and oxygen loss [18]. The spinel phase forms when the migrating Mn/Co cations are ordered in one-eighth (1/8) of the tetrahedral interstices located in the oxygen anion arrays. Note that this structural transformation is a gradual process. The cation ordering

degree can be represented by the amount of oxygen anion loss after annealing at different temperatures. The oxygen content evolution of the oxide nanocrystals, annealed at temperatures ranging from 200 to 500 °C, is plotted against the Curie temperature and the blocking temperature in Fig. 4c, d. It is interesting to note that the changes in T_C and T_B show a linear relationship with oxygen content loss (the cation ordering degree) for the Co-rich oxide nanocrystals annealed at different temperatures. The linear trend is not followed by the Mn-rich oxide nanocrystals, but major increments in T_C and T_B were detected for the Mn-rich oxide nanocrystals annealed at 400 °C for 5 h. The present experimental results show clear evidence of strong correlation between the magnetic properties and the cation ordering degree in the annealed Mn–Co–O nanocrystals.

It is well recognized that the magnetic moments of Mn/Co cations are rather sensitive to the cation interstitial occupancies in oxygen anion arrays. For instance, in the Co_3O_4 spinel structure, only Co^{2+} cations in the tetrahedral sites possess a magnetic moment. Co^{3+} cations in the octahedral sites have no permanent magnetic moment due to large crystal field splitting of the 3d orbitals by the octahedral crystal field [22]. Pei et al. also showed that for Mn-doped β-Ga_2O_3, the calculated magnetic moment of Mn cations occupying the tetrahedral interstices (3.467 μ_B/Mn) is much higher than the octahedral Mn occupancies (1.886 μ_B/Mn) [23]. Thus, the relationship between the cation ordering and magnetic properties in the annealed Mn–Co–O nanocrystals can be envisaged as follows. When

the annealing temperature is 100 °C, no cation ordering occurs; the Mn/Co cations and a large number of vacancies occupy the octahedral interstices randomly. This highly disordered state leads to a very small magnetic moment for the oxide nanocrystals, shown as the paramagnetic behavior in the insets of Fig. 2a, b. As the annealing temperature increases, more and more Mn/Co cations in the octahedral interstices have sufficient energy to overcome the energy barrier to order in the nearest tetrahedral interstices. This results in a rapid increase in the magnetic moment and, in turn, the onset of ferromagnetic behavior and the rapid increase of T_C and T_B for oxide nanocrystals annealed at 200–500 °C. The linear trend observed for the Co-rich oxide nanocrystals (Fig. 4c, d) indicates the predominant role of cation ordering on the corresponding magnetic properties. For the Mn-rich oxide nanocrystals, relatively faster grain growth induced by the fast diffusion rate of Mn cations in the oxygen anion arrays may account for the deviation from the linear trend (Fig. 4c, d) [24]. However, an unambiguous understanding will require systematic work to be conducted on a serious of electrodeposited Mn–Co oxide nanocrystals with different chemistries, including pure Co and Mn oxides.

Conclusions

The magnetic properties of the anodically electrodeposited Mn–Co oxide nanocrystals after annealing at temperatures ranging from 100 to 500 °C were investigated. When the annealing temperature is 100 °C, a paramagnetic behavior exists in both Mn-rich and Co-rich oxide nanocrystals. As the annealing temperature increases, ferromagnetic (FC) and superparamagnetic (ZFC) behavior can be observed. Curie temperature (T_C) and blocking temperature (T_B) increase dramatically with annealing temperature (200–400 °C), while the corresponding particle size growth of the oxide nanocrystals is rather small, especially for the Co-rich oxide nanocrystals. It was found that the changes in T_C and T_B show a linear relationship with the oxygen content loss (the cation ordering degree) for the Co-rich oxide nanocrystals annealed at different temperatures. The linear trend is not followed by the Mn-rich oxide nanocrystals, but major increments in T_C and T_B were detected for the Mn-rich oxide nanocrystals annealed at 400 °C for 5 h. These unique magnetic properties can be attributed to the magnetic moment changes induced by Mn/Co cation ordering from octahedral interstices to tetrahedral interstices in the annealed Mn–Co oxide nanocrystals.

References

1. Schmid G (2004) Nanoparticles: from theory to application. Wiley-VCH, New York
2. Sugimoto T (2001) Monodispersed particles. Elsevier, Amsterdam
3. Seo WS, Jo HH, Lee K, Kim B, Oh SJ, Park JT (2004) Angew Chem Int Ed 43:1115
4. Park JT (2005) Angew Chem Int Ed 44:2872
5. Zitoun D, Pinna N, Frolet N, Belin C (2005) J Am Chem Soc 127:15034
6. Park J, Kang E, Bae CJ, Park JG, Noh HJ, Kim JY, Park JH, Park HM, Hyeon T (2004) J Phys Chem B 108:13594
7. Na CW, Han DS, Kim DS, Park J, Jeon YT, Lee G, Jung MH (2005) Appl Phys Lett 87:142504
8. Xu R, Zeng HC (2004) Langmuir 20:9780
9. Park J, Kang E, Son SU, Park HMM, Lee K, Kim J, Kim KW, Noh HJ, Park JH, Bae CJ, Park JG, Hyeon T (2005) Adv Mater 17:429
10. Ghosh M, Biswas K, Sundaresan A, Rao CNR (2006) J Mater Chem 16:106
11. Ghosh M, Sampathkumaran EV, Rao CNR (2005) Chem Mater 17:2348
12. Zhang HT, Chen XH (2006) Nanotechnology 17:1384
13. Thota S, Kumar A, Kumar J (2009) Mater Sci Eng B 164:30
14. White MA, Ochsenbein ST, Gamelin DR (2008) Chem Mater 20:7107
15. Ozkaya T, Baykal A, Kavas H, Koseoglu Y, Toprak MS (2008) Physica B 430:3760
16. Wei WF, Chen WX, Ivey DG (2007) Chem Mater 19:2816
17. Wei WF, Chen WX, Ivey DG (2007) J Phys Chem C 111:10398
18. Wei WF, Chen WX, Ivey DG (2008) Chem Mater 20:1941
19. Bean CP, Livingston JD (1959) J Appl Phys 30:120S
20. Nagaev EL (2002) Colossal magnetoresistance and phase separation in manganites. Imperial College Press, London, p 317
21. Egilmez M, Chow KH, Jung J, Fan I, Mansour AI, Salman Z (2008) Appl Phys Lett 92:132505
22. Brankovic D, Jokanovic V, Babic-Stojic B, Jaglicic Z, Lisjak D, Kojic D (2009) J Phys Condens Matter 21:095303 11 pages
23. Pei GQ, Xia CT, Dong YJ, Wu B, Wang T, Xu J (2008) Scr Mater 58:943
24. Reed J, Ceder G (2004) Chem Rev 104:4513